International Symposium on the Conservation of Monuments in the Mediterranean Basin

(2024)

Proceedings of the 11th MONUBASIN (2024)

Protection coatings for stone monuments and artefacts of cultural heritage made of calcitic materials

Panagiota D. Natsi, Andreas Tzachristas, Varvara Sygouni, Christakis A. Paraskeva, Petros G. Koutsoukos

doi: 10.12681/monubasin.8336

Protection coatings for stone monuments and artefacts of cultural heritage made of calcitic materials

Panagiota D. Natsi, *Department of Chemical Engineering*, University of Patras, Karatheodory 1, 26504 Patras, Greece, *Foundation for Research and Technology-Hellas/Institute of Chemical Engineering Sciences (ICE-HT)*, Stadiou str., Platani, 26504 Patras, Greece

Andreas Tzachristas, *Department of Chemical Engineering*, University of Patras, Karatheodory 1, 26504 Patras, Greece

Varvara Sygouni, *Department of Chemical Engineering*, University of Patras, Karatheodory 1, 26504 Patras, Greece

Christakis A. Paraskeva, *Department of Chemical Engineering*, University of Patras, Karatheodory 1, 26504 Patras, Greece

Petros G. Koutsoukos, *Department of Chemical Engineering*, University of Patras Karatheodory 1, 26504 Patras, Greece, *Foundation for Research and Technology-Hellas/Institute of Chemical Engineering Sciences (ICE-HT)*, Stadiou str., Platani, 26504 Patras, Greece

Abstract. The degradation of marble monuments and statues is an ever-growing concern due to increased industrialization, extensive urban development, and persisting environmental quality problems. Preservation of the built cultural heritage and artefacts necessitates the development of novel materials and methods in order to increase their resistivity against the detrimental impacts of atmospheric water and pollutants. Over the past few decades, numerous protective coatings have been introduced to ensure the integrity of cultural heritage and prevent their degradation by reducing the rates of building materials deterioration. Protective coatings designed for cultural items are generally expected to adhere to established restoration standards, including transparency, reversibility, compatibility with the surface, long-term durability, straightforward synthesis, cost-efficient maintenance, and non-toxicity. Among coatings most often used for the protection of calcareous stone, poly acrylates and nanoparticles of metal oxides play significant roles in conservation and restoration activities. Graphene derivatives, including graphene oxide (GO), have garnered significant attention as protective coatings. In this study, we have studied graphene oxide-based structures as potential coatings for historical monument protection. Specifically, the resistance to dissolution of Dionysos marble (DM) specimens (1.5 x 1.5 cm x cm) were treated with Polyacrylic acid, MW 2000 (PAA2000), Hydroxy ethylidene, -1-1 phosphonic acid, sodium salt (HEDP) solutions and with GO suspension. DM, consists mainly of calcite (>98% w/w). All compounds tested for the treatment of DM, possessed functional groups capable of interactions with calcitic marble surfaces. The specimens were equilibrated with the solutions and suspension as follows: 2-5x10^{-5} mol/L for PAA and HEDP 2x10^{-5}-5x10^{-4} % w/v GO suspensions in water. Equilibration was done by immersing DM test slabs in the solutions and the suspension in 50 mL vials, capped and rotated end over end to ensure homogeneity for 24 hours at 25^{0}C. Past equilibration, the specimens were rinsed with triply distilled demineralized water and air dried. The samples were mounted into special holders in special reactors, allowing the flow of calcium carbonate unsaturated solutions (σ=0.89, pH 6.50) with a flow rate of 4.5 mL·h^{-1} in contact with both specimen surfaces. From measurements of pH and calcium concentration at the outlet of the reactors, the rates of dissolution of the specimens for each treatment tested were calculated. It was found that the equilibration of the marble specimens with GO suspensions was the most efficient, yielding a dissolution rate of 70% lower in comparison with the respective of the untreated marble. PAA-treated specimens did also retard the rate of dissolution of marble but to a less extent (ca. 30%). HEDP treatment was ineffective in retarding the dissolution rate of the DM specimens, possibly because of the enhancement of the calcitic material solubility in the presence of HEDP or because of structural rearrangement of the adsorbed phosphonate species on DM calcitic grains.

Proceedings of the 11th International Symposium on the Conservation of Monuments in the Mediterranean Basin, 17-19 of June 2024, Athens, Greece
https://doi.org/10.12681/monubasin.8336

Keywords: calcitic materials, dissolution, kinetics of coatings, effect of Keyword.

1 Introduction

The deterioration of the built heritage associated with the historical and cultural heritage threatens the loss of social identity and its legacy to future generations. Pieces of artwork kept indoors are exposed to controlled conditions in which environmental parameters like relative humidity, temperature, and light are monitored and/or controlled. Monuments of the built heritage and artefacts, mostly made from limestone and dolomitic or calcitic marbles [1] and exposed to atmospheric conditions, are threatened by weathering damages because of direct contact with wet precipitation. The problem is intensified in the presence of acidic pollutants and/or bacterial activity, which results in locally acidic conditions. [1]. Relatively easy quarrying, cutting, and carving make marble and limestone ideal for the construction of buildings and artifacts. However, these materials are prone to physical and chemical damage upon long-term exposure to environmental conditions.

Over the recent decades, a variety of protective coatings have been developed for the preservation of the integrity of the monuments, including the built heritage, aiming at reducing their rate of deterioration because of dissolution, which eventually leads to their complete destruction. Coatings for use in the conservation processes of monuments and artefacts should conform to certain criteria. They should ensure Transparency, reversibility, compatibility with the surface, long life, easy composition, low cost, and lack of toxicity [2]. In addition to the aesthetic aspect, the original appearance of archaeological or artistic objects should remain unaltered, and in case of corrosion (photooxidation - yellowing), the corrosion products should be removed without affecting the surface itself [3].

Significant advances have been achieved in coating science and technology over the past 30 years. Limestone and marble are sedimentary and metamorphic minerals respectively, the main component of which is calcite ($CaCO_3$). Contact of calcitic building materials with water can be dangerous because chemical dissolution leads to mechanical problems and the growth of microorganisms, such as mold, into the stone [5]. Biodegradation, based on activities of living organisms (fungi, bacteria, and algae), is an additional problem often associated with chemical deterioration and causes changes on the surface of the monument [6].

A wide range of acrylic polymer coatings have been used for limestone preservation against chemical and biological degradation for the last 50 years [7], mostly ethyl methacrylate (EMA) and poly (methyl methacrylate) (PMMA). For the same purpose, nanocomposites of TiO_2 with silane coatings [8], rendering resistance in water accumulation and photodegradation on stone building materials, have been applied. It should be noted that, in some cases, the formation of biofilms may act protectively for monument stones [9].

The majority of coatings applied to limestone monuments are considered as a short-term solution that needs regular inspection and re-application. The development of novel, effectively protective, and long-lasting, low-cost treatments, which can easily be applied both in portable and built heritage monuments, is needed. Graphene derivatives emerge as a possible solution [10]. From the graphene compounds family, relatively hydrophilic and chemically adaptable graphene oxide (GO) dispersions in water may be applied in the form of coatings for the protection of limestone and marble [11]. GO coatings were found to be effective in considerably limiting the deterioration of carbonated stones and degradation upon contact with water [12].

In this study, the effectiveness of the GO coatings, formed by deposition from aqueous colloidal suspensions on Dionysus marble (DM), a calcitic building material, can provide protection from dissolution upon contact with aqueous solutions undersaturated with respect to calcite. This is often the situation when monuments constructed from marble and/or calcitic limestone are exposed to wet precipitation. The study was done simulating the dissolution process at different conditions: stirred undersaturated solutions at constant pH, in small reactors in which DM slabs were exposed to calcium carbonate solutions undersaturated with respect to calcite, flowing at various flow rates, and in microchannels in which changes of a linear dimension of the DM calcitic crystals were monitored directly in a microchannel using snapshots from a video-camera. The effect of the GO coatings was compared with other coatings developed on DM treatment with poly acrylic acid (PAA) and 1-Hydroxyethylidene-1,1-diphosphonic acid (HEDP). The present work may be considered preliminary, proof-of-concept work for the evaluation of the functionality of novel coatings.

2 Experimental Section

The resistance to dissolution of DM specimens (1.5 x 1.5 cm x cm slabs) and powdered material was studied following treatment of the solids with polyacrylic acid, MW 2000 (PAA2000), Hydroxy ethylideno-1-1diphosphonic acid, sodium salt (HEDP) solutions and with graphene oxide (GO) suspensions ($5x10^{-4}$ w/v). The pH of the PAA and HEDP stock solutions and of the GO suspensions was adjusted to 6.8-7.0 with the addition of standard NaOH or HCl solutions, as needed. The DM samples (powder or slabs) were in contact with stirred calcium carbonate solutions saturated with respect to calcite at a constant temperature, 25 C in batch reactors. The desired concentrations of the test compounds in the saturated solutions were adjusted with the appropriate volume of the respective stock solutions and the suspension. The suspensions of DM in the presence of the test compounds were allowed to equilibrate for 5 days. Next, the solids were separated from the aqueous phase; they were washed with water and air-dried for 24h. The dried solids were used for the measurement of the rates of dissolution in calcium carbonate solutions undersaturated with respect to calcite (Fig.1). Table 1 summarizes the names of the substrates based on different treatments.

Table 1. Substrates treatment before dissolution study.

Substrate		Treatment solution
Powder	**DM1**	*Without treatment*
	DM2	*PAA2000 2×10^{-5} M*
	DM3	*HEDP 2×10^{-5} M*
	DM4	*GO 5×10^{-4} % w/v*
Specimens	**DMB**	*Without treatment*
	DMP	*PAA2000 2×10^{-5} M*
	DMH	*HEDP 2×10^{-5} M*
	DMGO	*GO 5×10^{-4} % w/v*

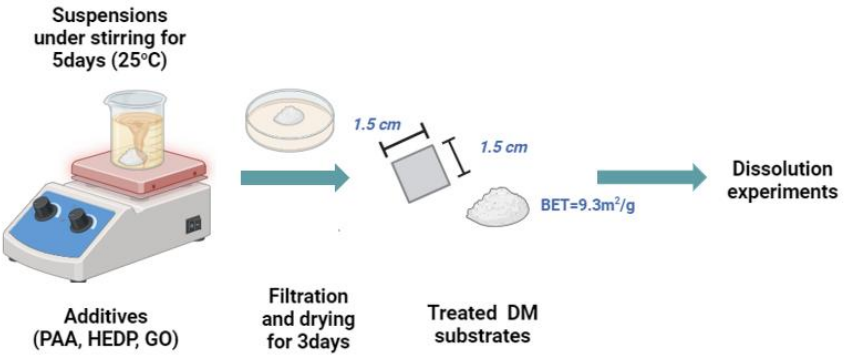

Fig. 1. Treatment process of marble substrates (powder or slabs) before dissolution kinetics measurements.

2.1 Dissolution experiments

Powdered DM with BET-specific surface area, measured with nitrogen, equal to 9.3 m^2 $g^{-1,}$ was used as reference material for the measurement of the rates of dissolution in calcium carbonate solutions undersaturated with respect to calcite. The rates of dissolution of DM treated with the test materials were measured as well (Table 1). The undersaturated solutions were prepared directly in a double wall batch reactor (V_R=200 mL) made of borosilicate glass (PYREX®) kept at 25.0 ± 0.1 °C with water from a thermostat, circulating between the walls of the reactor. The solutions were prepared by mixing accurately measured volumes of standard stock solutions of calcium chloride and sodium bicarbonate. Calcium chloride stock solutions were prepared from crystalline $CaCl_2 \cdot 2H_2O$ and standardized with atomic absorption spectrometry (AAS, Perkin Elmer AAnalyst 300) and by titrations with standard EDTA solutions with murexide indicator. Sodium bicarbonate stock solutions were prepared fresh before each experiment from the respective solid and dried overnight at 65°C. The final concentrations of calcium chloride and sodium bicarbonate in the undersaturated solutions was 1.25 mM, and the ionic strength was adjusted to 0.15 M with the addition of standard NaCl solution as needed. 1M standard

stock solutions were prepared from accurately weighed solid and dried overnight at 65°C, without any further standardization. The pH of the undersaturated solutions was adjusted to 6.50 with a standard 0.1 N HCl solution. Following pH adjustment, an accurately weighed powdered solid (10 mg) was introduced into the undersaturated solutions. As a result of the dissolution of calcium carbonate, the pH of the solution increased. The dissolution of calcium carbonate is described by the reaction:

$$CaCO_3 + H_2O \leftrightarrow Ca^{2+} + HCO_3^- + OH^- \quad (1)$$

Changes in the solution pH as small as 0.005 pH units triggered the addition of standard HCl solution (0.1 M) from the precision syringe of a computer-controlled pH stat system. The dissolution process was monitored at constant pH. Samples were withdrawn and filtered through membrane filters (Sartorius, 0.2 μm), and the filtrates were analyzed for total calcium, by AAS. The experimental set-up for the dissolution experiments is shown in Fig.2.

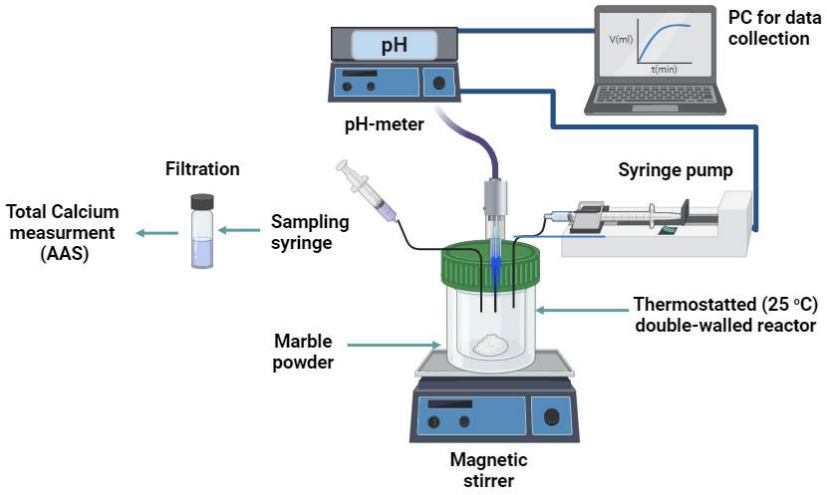

Fig. 2. Experimental setup for dissolution experiments at constant pH (pH- stat method).

2.2 Dissolution of marble slabs in thermostated small volume reactors

The dissolution of marble slabs was investigated in small double-walled reactors made of polyamide volume totaling ca. 10 mL, in which the marble slabs with dimensions ca. 1.5 cm x 1.5 cm were immobilized in special holders. The temperature in the small-volume reactors was kept at 25.0 ± 1.0 °C by water circulating from a thermostat. The flow rate of the undersaturated solution was adjusted to 4.5 $mL \cdot h^{-1}$ by using a syringe pump, and the duration of each experiment was 3 days. Samples were withdrawn at different times, with higher frequency at the initial steps, slowing down as the dissolution proceeded to equilibrium, filtered, and the filtrates were analyzed for total calcium concentration with AAS. Moreover, the pH of the solution was measured at the outlet of the reactor as a function of time. The pH-time profiles were used to monitor the dissolution process. The morphology of the marble slabs at the end of each dissolution experiment was investigated with scanning electron microscopy (SEM, Zeiss, Leo Supra 35). A schematic layout of the experimental setup and procedure is given in Fig. 3.

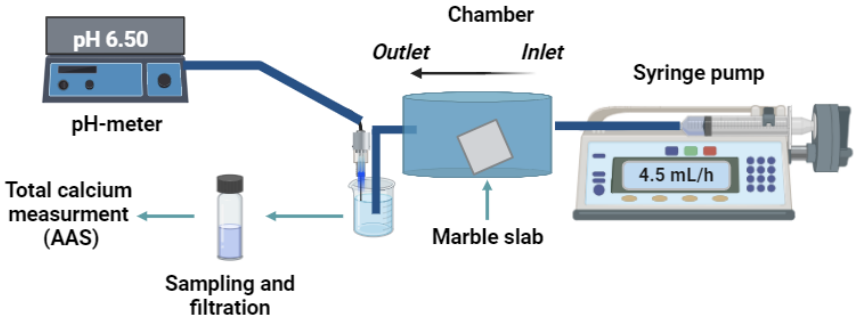

Fig. 3. Experimental setup for dissolution experiments of marble slabs with flowing undersaturated solutions.

Additional dissolution tests were done in porous media simulators made of Plexiglas®. The linear channel used had dimensions of 6 cm length, 1 mm width, and 0.3 mm depth. Grains of the marble specimens investigated were introduced in the microchannel. The undersaturated solutions were introduced in the channel with a syringe pump, which ensured a constant flow rate (0.2-0.5- 1 $mL \cdot h^{-1}$). The solution flow rate was low inside the channel, and the Reynolds number values calculated were 0.095, 0.238, and 0.477 for flow rates 0.2, 0.5, and 1 $mL \cdot h^{-1,}$ respectively. At these values, the flow was laminar and was sufficient to ensure the stability of the position of the introduced calcite crystallites (with and without treatment).

Optical monitoring of the marble substrates was done using an optical microscope (Zeiss, microscope with camera), which was connected to a digital camera (AXIS 223M Network Camera). Thus, it was possible to record and store photograph snapshots at regular intervals (every 30 min) on a computer through special data recording software (AXIS Camera Station). Past the end of each experiment, the photograph snapshots were processed with image processing software (ImageJ®). From the processing of the snapshots, data concerning size changes of the marble grains as a function of time were obtained. The experimental setup described is schematically presented in Fig.4.

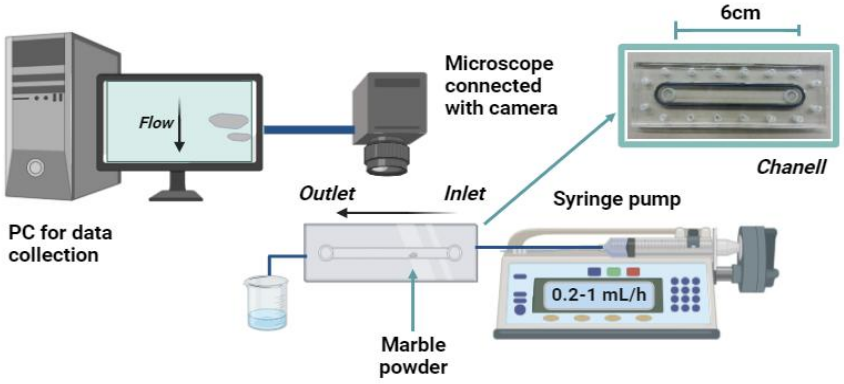

Fig. 4. Experimental setup for dissolution experiments of DM powders at different flow rates of the calcium carbonate solutions undersaturated with respect to calcite.

3 Results and Discussion

3.1 Dissolution experiments

The dissolution rates of DM were measured in solutions undersaturated with respect to calcite (which is the main chemical component of DM). The driving force for dissolution at constant temperature depends on the solution saturation ratio, SR, defined as:

$$SR = \frac{(Ca^{2+})(CO_3^{2-})}{K_s^o} \quad (2)$$

Where parentheses correspond to the activities of the ions enclosed and K_s^o is the thermodynamic solubility product of calcite. In the case of undersaturated solutions SR<1. For solutions saturated with respect to calcite SR=1. The activities of the free ions were calculated from the total concentrations of the main components of the solutions using PHREEQC® equilibrium calculations software, v. 3.3.12.12704 [21]. The relative undersaturation, σ, of the solutions, is defined by equation (4):

$$\sigma = 1 - SR^{1/2} \quad (3)$$

The relative undersaturation of the working solutions with respect to calcite was 0.99. The dissolution process was monitored as a function of time at a constant temperature of 25.0 ± 0.5 °C in a batch, magnetically stirred reactor. pH was kept constant at 6.50 at ionic strength 0.15 M NaCl.

In Fig.5, typical plots of the volume of standard solution of 0.1N HCl solution added to maintain the solution pH during solution, are shown. The solution undersaturation decreased as a function of time, which explains the trend shown on the pH-time profiles. The rates of dissolution were proportional to the respective rate of additions of acid solution.

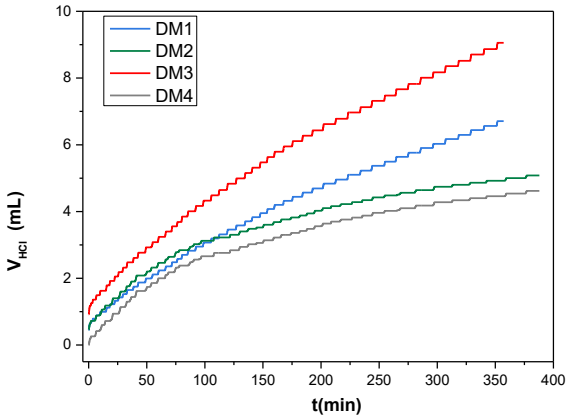

Fig. 5. Dissolution of DM in undersaturated calcium carbonate solutions (σ= 0.99, SR= 1x10^{-3}), 25 °C, pH 6.50, 0.15 M NaCl; (-) Without treatment -Blank (DM4); (-) PAA treatment (DM1); (-) HEDP treatment (DM2); (-) GO treatment (DM3).

The total calcium concentration as a function of time profiles corresponding to the volume additions as a function of time (Fig. 5) are shown in Fig. 6.

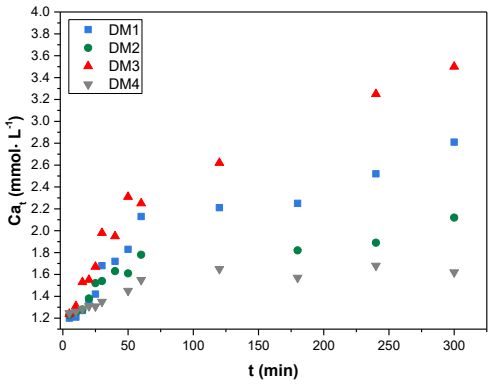

Fig. 6. Calcium concentrations (Ca_t) from dissolution of DM in undersaturated calcium carbonate solutions (σ= 0.99), 25 °C, pH 6.50, 0.15 M NaCl; (■) Without treatment -Blank (DM4); (●) PAA treatment(DM1); (▲) HEDP treatment (DM2); (▼) GO treatment (DM3).

The rates of dissolution of the respective DM specimens were calculated from the total calcium- time profiles according to equation (4) using data from the first 60 min following the contact of the solids tested, with the undersaturated solutions:

$$Rate\ of\ Dissolution, R_D = \left|\frac{d[Ca_t]}{dt}\right|_{t=0} \quad (4)$$

The calculated initial rates, are summarized in Table 2 and in the form of a plot in Fig. 7.

Table 2. Dissolution rates of DM powdered samples at constant pH; σ= 0.99, 25 °C, pH 6.50, 0.15 M NaCl

Substrate	Dissolution Rate* (/×10^{-5} mol·m^{-2}·min^{-1})
DM1	3.58
DM2	2.15
DM3	4.95
DM4	1.14

**The dissolution rate was calculated per BET specific surface area.*

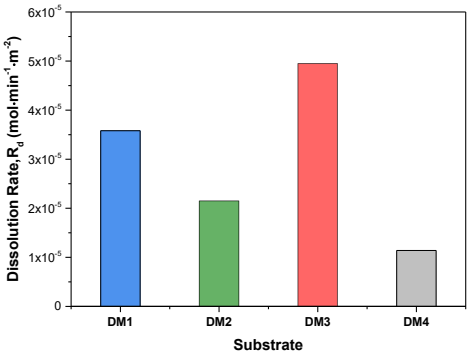

Fig. 7. Dissolution rates of DM with different treatments in calcium carbonate solutions undersaturated with respect to calcite (σ= 0.99); DM1: untreated; DM2: PAA treated; DM3: HEDP treated; DM4: GO treated; 25 °C, pH 6.50, 0.15 M NaCl

The dissolution rate of the DM with GO deposits (DM4) was the lowest in comparison with all other treatments. The rate was almost 70% lower than the rate of the untreated (blank) material. It is possible that the GO coating slows down the dissolution of marble because of the formation of protective film, which blocked effectively the active sites of dissolution on the surface of the DM material. The high concentration of oxygen-containing functional groups of GO (-COOH, -OH, -O-) possibly interact electrostatically with Ca^{2+} and Mg^{2+} cations of the DM, forming surface complexes with GO. PAA treatment reduced the rate of dissolution by 30% in comparison with the untreated DM. HEDP treatment accelerated significantly (ca. 20%) the dissolution in comparison with the respective for the untreated specimens.

The surface coverage by graphene oxide, the morphology of marble powder treated with different concentrations of GO suspensions was investigated by SEM. As shown in Fig.8(a), the grains of powdered DM treated with the GO suspension (5x10^{-4} %w/v) were partly coated. The presence of grains completely covered with GO layers (Fig.8(b)), was confirmed by EDX line scan analysis (Fig.8(c)).

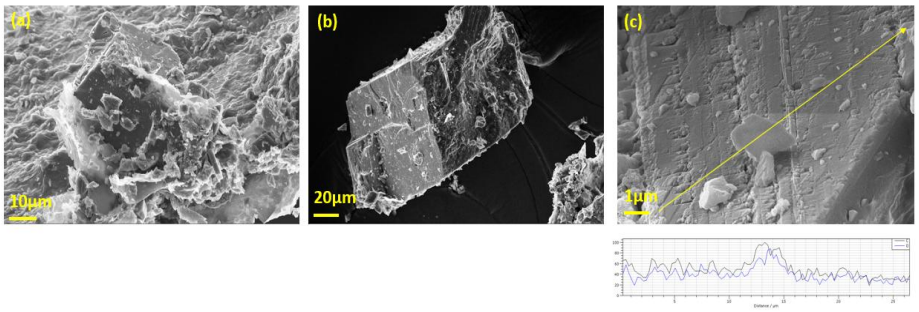

Fig. 8. SEM photos of marble grains following equilibration with GO suspensions (5x10^{-4} %w/v) for five days.

DM powders, equilibrated with GO suspensions with lower GO content (5x10^{-5} %w/v), resulted in the formation of uniform coating on marble calcitic grains (Fig.9).

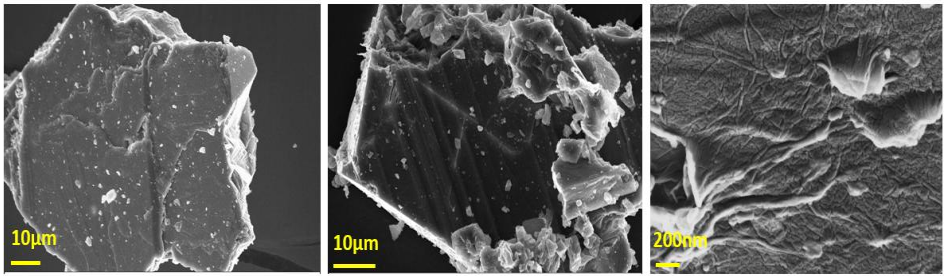

Fig. 9. SEM photos of marble grains past equilibration with GO suspensions (5x10^{-5} %w/v) for five days.

The highest dissolution rates were obtained for the HEDP-treated powdered DM (DM3) (Fig.7). In most publications, referred that HEDP form complexes with calcium cations in different proportions of Ca^{2+} and phosphonate ions (1:1 or 1:2) in p H 8-8.5 [13]-[15]. This leads to the formation of a

protective film, which tends to reduce dissolution rates. However, in the present work at the acid pH 6.5, rates of dissolution were higher in comparison with the respective DM without any treatment. This acceleration may be explained based on the calcium phosphonate adsorbed layer re-structuring on the surface over a period of time, resulting in the exposure of active dissolution sites of the mineral substrate [16].

The measured rate of dissolution for marbled treated with PAA (DM2), was lower in comparison with the corresponding to the untreated DM. PAA polymers have already been used in the past for marble and limestone protection due to their good adhesion performance [3],[17].

3.2 Dissolution of marble slabs

DM slabs, both untreated and treated (Table 1), were exposed to the flow of calcium carbonate solutions undersaturated with respect to calcite (σ=0.99) at a flow rate of 4.5 ml/h. The increase of pH measured at the outlet of the microchannel confirmed their dissolution. pH change over a period of 5 hours is shown in Fig.10. In the case of G- coated DM slabs (DMGO), pH increased at a slower rate during dissolution in comparison with the respective in the untreated DM (DMB). The highest increase and rate of increase was observed in the case of HEDP treatment (DMH).

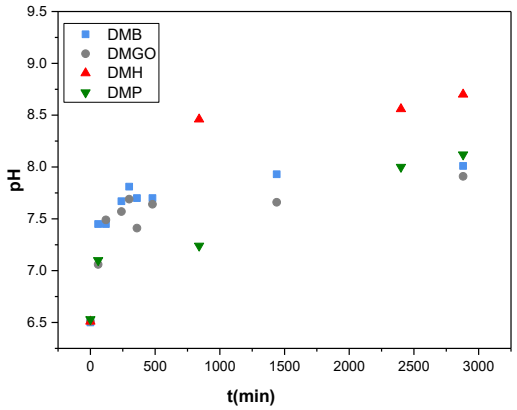

Fig. 10. pH changes as a function of time, of the calcium carbonate solutions undersaturated with respect to calcite during the dissolution of DM slabs; flow rate of the undersaturated solutions 4.5 mL·h^{-1}; ($\sigma_{initial}$= 0.99), 25 °C, 0.15 M NaCl; (■) Without treatment -Blank; (▼) PAA treatment; (▲) HEDP treatment; (●) GO treatment.

In addition to pH measurements in the undersaturated solutions, the calcium concentration was measured as well in the outlet from the reactor. As shown in Fig.11, calcium concentration also increased in all cases. The highest increase of calcium concentration in the solutions was observed for HEDP and the lowest for GO-treated DM slabs. The initial rates of the dissolution of the DM slabs were assessed from the variation of total calcium during the first 60 min of the dissolution process presented in (Fig.12), which was rather fast. From the calcium concentration measurements, the rate of dissolution was calculated for the first hour. The dissolution rates of the DM slabs calculated for both untreated and treated are shown in Fig.13. The main difference between these experiments and the pH-stat experiments (DM powders) was that the rate in this case was calculated per geometrical unit surface area of the slabs.

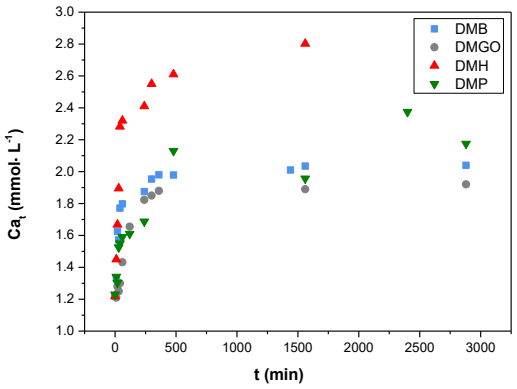

Fig. 11. Dissolution of DM slabs in calcium carbonate solutions undersaturated with respect to calcite ($\sigma_{initial}$= 0.99); Total calcium concentration in the solutions during dissolution as a function of time. 25 °C, 0.15 M NaCl; Flow rate=4.5 mL·h^{-1}; (■) Without treatment -Blank; (▼) PAA treatment; (▲) HEDP treatment; (●) GO treatment.

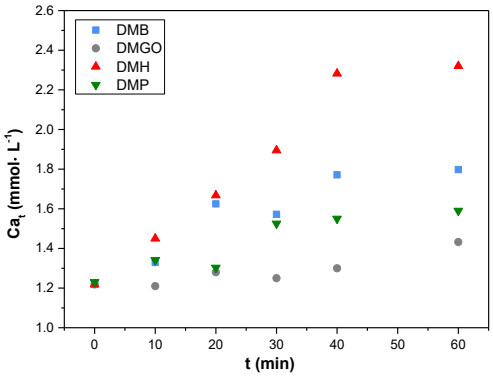

Fig. 12. Calcium concentrations (Ca_t) from Dissolution of DM slabs underflow of the calcium carbonate solutions undersaturated with respect to calcite ($\sigma_{initial}$= 0.99). Plot of the total calcium (Ca_t) concentrations in the undersaturated solutions as a function of time for the first 60 min of the dissolution process; 25 °C, 0.15 M NaCl; Flow rate=4.5 mL·h^{-1}; (■) Without treatment -Blank; (▼) PAA treatment; (▲) HEDP treatment; (●) GO treatment.

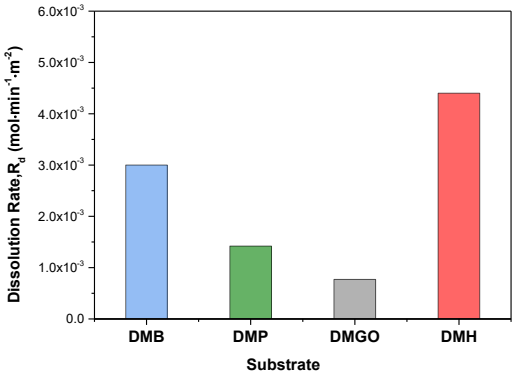

Fig. 13. Dissolution rates of DM slabs without and past treatments with solutions of PAA, HEDP, and GO suspensions in solutions undersaturated with respect to calcite ($\sigma_{initial}$= 0.99), underflow; 25 °C, 0.15 M NaCl; Flow rate=4.5 mL·h^{-1}. DMB: blank; DMP: PAA treated; DMGO: GO treated; DMH: HEDP treated.

The rates of dissolution of DM slabs showed the same trend as the measurements of dissolution of powdered DM at the pH-stat experiments, suggesting that both experimental models are reliable for conducting rapid tests for materials candidates for the protection of building materials of the cultural heritage. More specifically, the highest rates of dissolution were found for the treatment of DM with HEDP and the least for GO-treated specimens. The dissolution rates of the DM slabs coated with GO (DMGO) yielded the lowest rates of dissolution, being almost 74% lower than the respective for the untreated specimens. The efficiency of GO coatings may be explained by the fact that at pH ca.7.0, at which treatment is done, GO has a high negative charge because of the almost complete ionization of the -COOH groups and the positive surface charge of calcite [18]. Electrostatic interactions contribute to the formation of a coating that effectively blocks the active sites for dissolution. The results obtained are encouraging for the use of GO as a protective coating for marble, in agreement with similar studies [19], [20].

The effect of dissolution on the morphology of marble slabs was examined by SEM. The morphology of the DM slabs before and after dissolution is shown in Fig.14(a) and (b). Surface deterioration (compared with flat parts of the surface of the marble before dissolution) was observed with the formation of pits on the specimen surface, with sizes between 50 to 100 nm or even > 200 nm. For the specimen treated with PAA (DMP) (Fig.14(c)), as may be seen, PAA provides a more uniform coating, which, however, does not seal the pores on the specimen surface. In the HEDP-treated specimen (DMH), the development of pits was apparent past dissolution. The appearance of some needle-like and plate-like "transparent" crystallites (Fig.14(d)) suggested the formation of Ca-HEDP or Mg-HEDP. This was supported by the results of the EDX analysis. Finally, for the treatment of DM with GO (DMGO), the surface coverage of the slab seemed to be low, with dark flakes of GO spreading all over the surface. Past dissolution of the GO treated specimens surface damages and pit formation was drastically reduced.

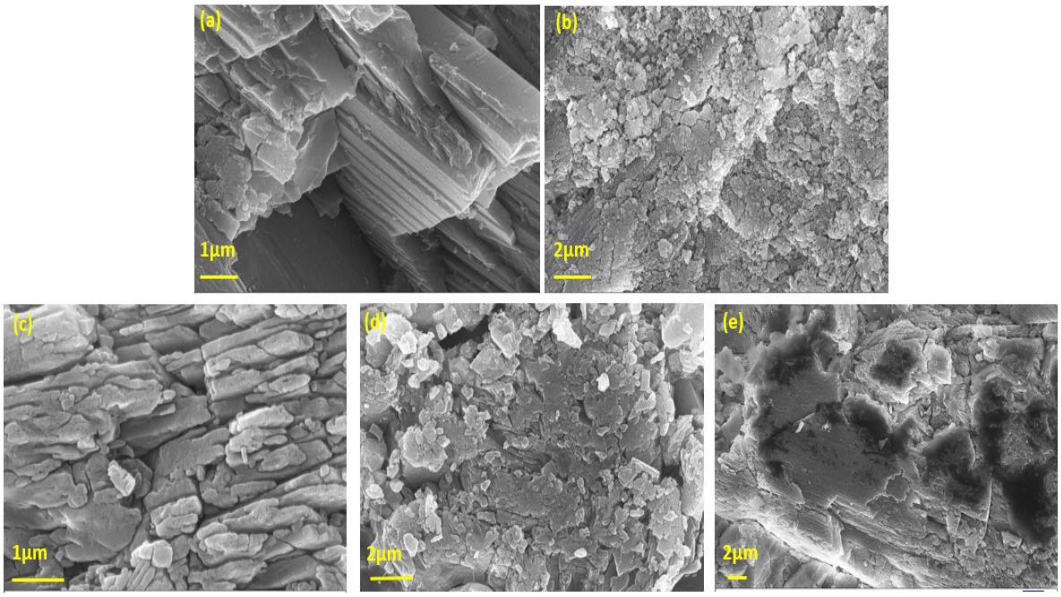

Fig. 14. Dissolution of DM in calcium carbonate solutions undersaturated with respect to calcite $\sigma_{initial}$= 0.99). SEM pictures of the morphology of the surface of DM slabs (**a**) Untreated marble, DMB (**b**) DMB, (**c**) DM treated with PAA, DMP, (**d**) DM treated with HEDP, DMPH and (**e**) DM treated with GO suspension, DMGO; 25 °C, 0.15 M NaCl; Flow rate=4.5 mL·h^{-1}.

3.3 Dissolution of DM grains in microchannel reactors

Powdered DM coated with GO (DM4) was brought in contact with the undersaturated solution, flowing at rates in the range of 0.2-1.0 mL·h^{-1}. The dissolution process was followed by monitoring changes in a linear dimension, x, of the DM grains. The (linear) dissolution rates, $\bar{R}_{diss}$ were calculated from equation (5):

$$\bar{R}_{diss}[m \cdot min^{-1}] = \frac{dx}{dt} \quad (5)$$

At flow rates of the undersaturated solutions in the microchannel 0.2 and 1 mL·h^{-1}, no change in grain size was observed, even after 5 days. It is possible that the GO film covering the DM grains observed completely inhibited the dissolution process. Considering that a limited number of DM grains were monitored (<10) in an equal number of experimental runs, it is clear that a significantly larger number of observations is needed. Typical pictures of DM grains inside the microchannel in contact with the undersaturated solutions are shown in Fig.15

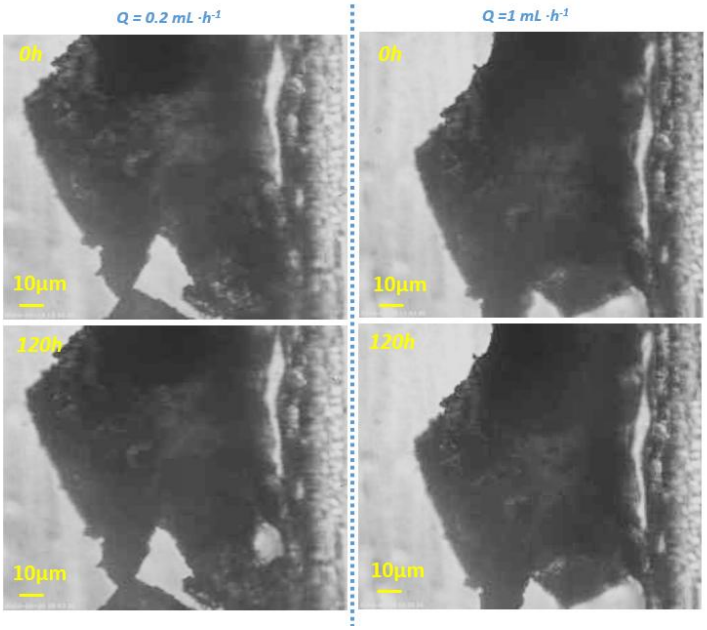

Fig. 15. Sequence of images captured during dissolution of GO coated DM grain (DM4) underflow of undersaturated solution; $\sigma_{initial}$= 0.99, 25 °C, 0.15 M NaCl; Flow rate=0.2 and 1 mL·h^{-1}.

At a higher flow rate (0.5 mL·h^{-1}), as may be seen in the optical microscope pictures shown in Fig.16, changes of one dimension of a typical DM grain as a function of time could be clearly seen and measured. Specifically, the initial and final DM grain sizes measured were 98.65 µm and 64.17 µm (Fig.16), respectively. This decrease in the magnitude of the characteristic dimension was gradual, and its variation as a function of time reached a plateau value corresponding to the final size of the characteristic linear dimension selected, as may be seen in Fig.16. Reaching the plateau needed 69h.

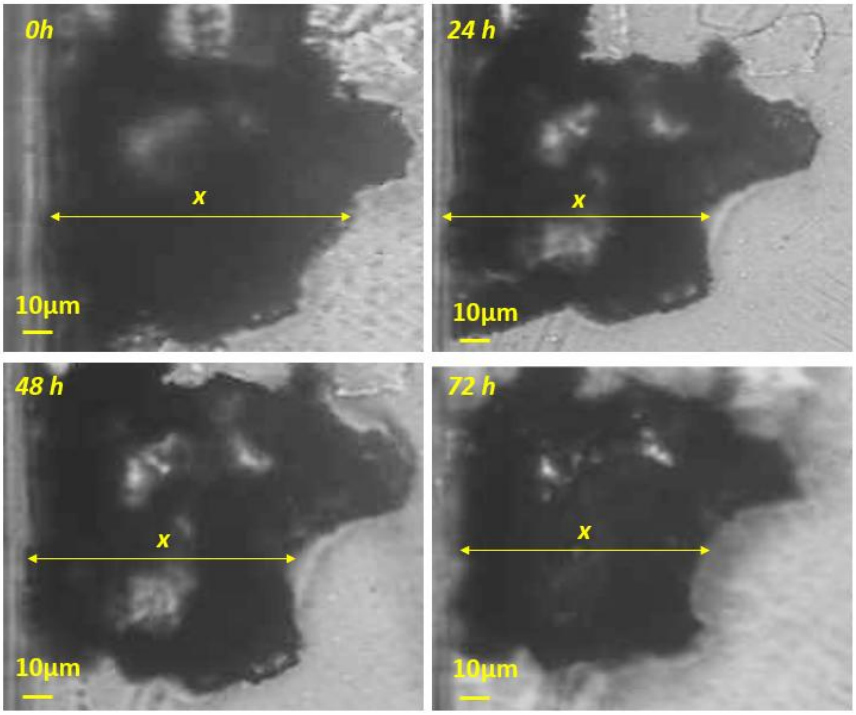

Fig. 16. Sequence of images captured during dissolution of GO coated DM grain (DM4) under flow of calcium carbonate solution undersaturated with respect to calcite; $\sigma_{initial}$= 0.99, 25 °C, 0.15 M NaCl; Flow rate=0.5 mL·h^{-1}.

The initial rate of dissolution calculated from the grain size change, was equal to 0.46 μm·h^{-1} (or 7.7×10^{-9} m·min^{-1}). The relationship between the linear rate of dissolution, $\bar{R}_{diss}$ with the respective mass loss rate, R_{diss}, expression is related with Eq. (6) [21]:

$$R_{diss}\,[Kg \cdot m^{-2} \cdot min^{-1}] = SF \cdot \rho_{calcite} \cdot \bar{R}_{diss} \tag{6}$$

In Eq. (6), *SF is a shape factor, which for spheres and cubes is 1, and c is* the density of calcite (the main chemical component of DM = 2711 Kg·m^{-3}). From Eq. (6) the mass loss rate of dissolution is equal to 2.1x10^{-4} mol·m^{-2}·min^{-1}. The calculated value is one order of magnitude higher thnt the rate of dissolution obtained from the pH-stat experiments at pH 6.50, where the initial rates of dissolution of powdered DM were measured. The reason for this discrepancy may be the difference in particle size. The smaller the particle size, the faster it is expected to dissolve. However, a significantly larger number of crystallites should be measured to establish a relationship between the two methods of measurement of the rate of dissolution.

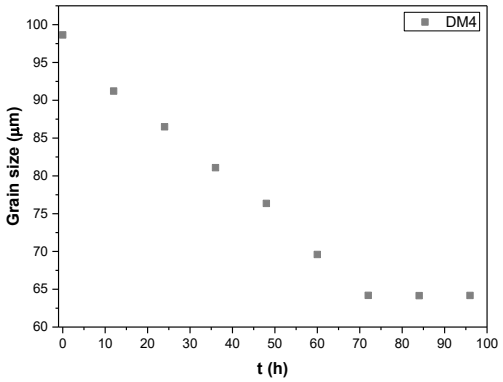

Fig. 17. Dissolution of selected GO-coated DM grain (DM4). Grain linear dimension size change as a function of time; $\sigma_{initial}$= 0.99, 25 °C, 0.15 M NaCl; Flow rate=0.5 mL·h^{-1}.

As may be seen in Fig. 17, the rate of dissolution is constant for a time period of ca. 65 hours. Past this time, the dissolution process ceased apparently reaching near saturation solubility. The constancy of the rate of dissolution is possible that is due to the fact that changes in the solution saturation with respect to calcite were minimal (at the slowest flow rate tested, 0.5ml/h, the change in calcium concentration was ca. 2.5%, which is within experimental error). The higher the flow rate, the smaller the changes are expected, provided that the mechanism of dissolution remains the same. It may, therefore, be suggested that the number of active sites remains constant, leading to a constant rate of dissolution, which may be monitored for long time periods. Earlier work has shown that the dependence of the rate of dissolution of DM, R_{diss}, in calcium carbonate solutions undersaturated with respect to calcite, was first order with respect to the relative supersaturation with respect to calcite, $\sigma_{calcite}$, suggesting surface diffusion-controlled kinetics [13]:

$$R_{diss} = k_{diss}\sigma_{calcite} \tag{7}$$

In the present case of DM slabs, should the mechanism be mass transport controlled, it should be:

$$k_{diss} = \frac{D}{\delta} \tag{8}$$

In Equation (8), *D* is the diffusion constant of the diffusing growth units (of the order of magnitude of inorganic ions, Ca^{2+}, or CO_3^{2-}, i.e., simple multiples of 10^{-10} m^2·s^{-1}) and δ the thickness of the boundary layer around the DM grains [22]:

$$\delta = (5.74\mu m) * r^{0.145} * (\Delta\rho)^{-0.285} \tag{9}$$

In Eq. 9, r is the radius of dissolving DM grains (98.7 μm) and $\Delta\rho$, the density difference between DM grain and water (1.71 $g \cdot cm^{-3}$). Substituting in Eq. 9, we obtained the value δ=9.6 μm. The dissolution constant calculated from the respective rate value measured was 7.8×10^{-9} $m \cdot min^{-1}$. The value of D according to the measurements should, therefore, be 1.24×10^{-15} $m^2 \cdot s^{-1}$. The value is unrealistically low for mass transport. It may, therefore, be suggested that in the microchannel as well, the mechanism of dissolution of the DM grains was again controlled by surface diffusion. This implies that reduction of active sites for dissolution of DM grains results in the reduction of rates of dissolution, concomitant with the application of coatings, provided that their conformation allows blocking and thus reducing active sites for dissolution on the calcitic crystals of DM grains.

Clearly more work should be done in the investigation of the effect of flowrate on the kinetics of dissolution of DM over a rather wide range of undersaturation with respect to calcite.

4 Conclusions

DM powders and slabs were treated with two solutions of compounds possessing functional groups that may interact strongly, forming chemical bonds with calcitic materials and with a suspension of GO particles, which are deposited on DM by electrostatic interactions. The dissolution of DM was studied in calcium carbonate solutions undersaturated with respect to calcite at constant and/or variable pH in stirred batch reactors and in a microchannel and small flow-through reactor, respectively. The common conclusion from all measurements was that GO-coated DM yielded the lowest rates of dissolution, the reduction reaching as much as 60% in comparison with the untreated material. The microchannel reactor in which dissolution rates are monitored by video recording and/or by successive pictures taken as a function of time is a useful tool for screening the effect of various treatment agents for stone protection. HEDP and PAA low MW polymers were less efficient in reducing rates of dissolution in acid pH, although alkaline pH values have been reported as very efficient. Apparently, the extent of molecular ionization and of the conformation of these compounds on the surface of calcitic materials like DM is very important with respect to the protection of calcitic materials.

References

1. Punturo, R., Russo, L. G., Lo Giudice, A., Mazzoleni, P., Pezzino, A.: Building stone employed in the historical monuments of Eastern Sicily (Italy). An example: the ancient city centre of Catania. Environmental Geology (50), 156–169 (2006).
2. Sbardella, F., Bracciale, M. P., Santarelli, M. L., & Asua, J. M.L: Waterborne modified-silica/acrylates hybrid nanocomposites as surface protective coatings for stone monuments. Progress in Organic Coatings, 149, 105897 (2020).
3. Artesani, A., Di Turo, F., Zucchelli, M., Traviglia, A.: Recent Advances in Protective Coatings for Cultural Heritage–An Overview. Coatings 10, 217 (2020).
4. Mosca S., Artesani, A., Gulotta, D., Nevin, A., Goidanich, S., Valentini, G., Comelli, D.: Raman mapping and time-resolved photoluminescence imaging for the analysis of a cross-section from a modern gypsum sculpture. Microchemical Journal 139, 500–505 (2018).
5. Cultrone, G., Sebastián, E.: Laboratory simulation showing the influence of salt efflorescence on the weathering of composite building materials. Environmental Geology 56, 729–740 (2008).
6. Nuhoglu, Y., Oguz, E., Uslu, H., Ozbek, A., Ipekoglu, B., Ocak, I., Hasenekoglu, I.: The accelerating effects of the microorganisms on biodeterioration of stone monuments under air pollution and continental-cold climatic conditions in Erzurum, Turkey. Science of the Total Environment 364, 272–283 (2006).
7. Feller, R.L.: New solvent-type varnishes. Studies in Conservation 6, 171-175 (1961).
8. Munafò, P., Gofferdo, G.B., Quagliarini, E.: TiO2-based nanocoatings for preserving architectural stone surfaces: An overview. Construction and Building Materials 84, 201-2018, (2015).
9. Carter, N.E.A., Viles, H.A.: Bioprotection explored: The story of a little-known earth surface process. Geomorphology 67, 273–281 (2005).
10. Alrashed, M. M., Soucek, M. D., Jana, S. C.: Role of graphene oxide and functionalized graphene oxide in protective hybrid coatings. Progress in Organic Coatings 134,197-208 (2019).
11. Healy, B., Yu, T., da Silva Alves, D., Breslin, C. B.: Review of Recent Developments in the Formulation of Graphene-Based Coatings for the Corrosion Protection of Metals and Alloys. Corrosion and Materials Degradation 1, 296-327 (2020).

12. Antolvn-Rodrvguez, A., Merino-Maldonado, D., Juan-Valdıs, A., Gonzαlez-Domvnguez, J.-M., Fernαndez-Raga, M., Garcva-Gonzαlez, J.: Performance of graphene oxide as a water-repellent coating nanomaterial to extend the service life of concrete structures. Heliyon 10, e23969 (2024).

13. Kanellopoulou, D.G., Koutsoukos, P.G.: The Calcitic Marble/Water Interface: Kinetics of Dissolution and Inhibition with Potential Implications in Stone Conservation. Langmuir 19, 5691-5699 (2003).

14. Spanos, N., Kanellopoulou, D.G., Koutsoukos, P.G.: The interaction of diphosphonates with calcitic surfaces: understanding the inhibition activity in marble dissolution. Langmuir. 22(5), 2074-2081 (2006).

15. Ruiz-Agudo, E., Di Tommaso, D., Putnis, C. V., de Leeuw, N. H., Putnis, A.: Interactions between Organophosphonate-Bearing Solutions and (1014) Calcite Surfaces: An Atomic Force Microscopy and First-Principles Molecular Dynamics Study. Crystal Growth & Design 10(7), (2010).

16. Lupu, C., Arvidson, R.S., Luttge, A., Barron, A.R.: Phosphonate mediated surface reaction and reorganization: implications for the mechanism controlling cement hydration inhibition, Chemical Communication, 2354–2356 (2005).

17. Ocak, Y., Sofuoglu, A., Tihminlioglu, F., Böke, H.L: Protection of marble surfaces by using biodegradable polymers as coating agent. Progress in Organic Coatings 66(3), 213–220 (2009).

18. Somasundaran P. Agar G.E: The zero point of charge of calcite. Journal of Colloid and Interface Science, 24, 433-440 (1967).

19. Gonzalez-Campelo, D., Fernandez-Raga, M., Gomez-Gutierres, A., Guerra-Romero, M. I., Gonzalez-Dominguez, J.M.: Extraordinary Protective Efficacy of Graphene Oxide over the Stone-Based Cultural Heritage. Advanced Materials Interfaces 8(23), 2101012 (2021).

20. Martínez-García, R., González-Campelo, D., Fraile-Fernández, F.J., Castañón, A.M., Caldevilla, P., Giganto, S., Ortiz-Marqués, A., Zelli, F., González-Domínguez, J.M.,Fernández-Raga, M.: Performance Study of Graphene Oxide as an Antierosion Coating for Ornamental and Heritage Dolostone. Advanced Materials Technologies, 2300486 (2023).

21. Mullin, J. W.: Crystallization, 4th Edition. Butterworth Heinemann, Oxford, UK. 600, pp. page 236 (2001).

22. Nancollas, G.H., In vitro studies of calcium phosphate crystallization, in S.Mann, J.Webb, R.J.P. Williams (Eds.) Biomineralization, VCH, Weinheim, p.166 (1989)